13

SiC-Based Composites Sintered with High Pressure Method

Piotr Klimczyk
Institute of Advanced Manuacturing Technology
Poland

1. Introduction

Silicon carbide-based materials usually have high hardness (2500 – 2800 HV) and thus have superior wear resistance. Nevertheless, the tribological performance of SiC is determined by many factors, such as the grain size of mated materials or the reactions in the presence of oxygen and humidity in the surrounding atmosphere. For example, in unlubricated sliding, wear resistance of SiC ceramics can be greater in air than in inert atmosphere owing to thin soft oxide films reducing friction and local surface pressure. (Gahr et al., 2001; Guicciardi et al., 2007). The friction and wear properties of SiC materials (both in dry and lubricating conditions) have been studied extensively because they are used in applications like bearings, cylinder liners and mechanical seals (Murthy et al., 2004).

Silicon carbide-based ceramics have high melting point (~2500 °C), high thermal conductivity (43 – 145 W/m·K – depending on a temperature and phase composition), low thermal expansion (~4,5×10^{-6}·K^{-1}), and high temperature capability. Silicon carbide is a semiconductor which can be doped n-type by nitrogen or phosphorus and p-type by aluminium, boron, gallium or beryllium. Due to the combination of its thermal and electrical properties, SiC is applied in a resistance heating, flame igniters and electronic components. Relatively pure SiC has also an excellent corrosion resistance in the presence of hot acids and bases (Richerson, 2004).

Silicon carbide powder compacts are difficult to densify without additives because of the covalent nature of the Si–C bonds and the associated low self-diffusion coefficient. Therefore, Reaction Sintering (RS) in the presence of liquid silicon as well as Hot Isotactic Pressing (HIP) are frequently used to obtain a high quality, full dense SiC ceramics. Typical room temperature flexural strength of SiC-based materials is about 350-550 MPa. High-strength RS-SiC (over 1000 MPa in a 3-point bending test) was developed by controlling the residual Si size under 100 nm. (Magnani et al., 2000; Suyama et al., 2003). Silicon carbide ceramics have the ability to increase in strength with increase of temperature. It was reported that flexural strength of some kind of commercial SiC ceramic increase is from 413 MPa at the room temperature to around 580 MPa at 1800 °C (Richerson, 2004). For hot-pressed silicon carbide with addition of 0.15-1.0 wt% Al_2O_3, the high-temperature strength has been improved from 200 MPa to 700 MPa by decreasing the grain boundary concentration of both Al and O at 1500 °C (Kinoshita et al., 1997).

A favorable combination of properties makes SiC materials suitable for many engineering applications, including parts of machines and devices exposed to the abrasion, the high temperature, the corrosive environment, etc. A major disadvantage of SiC ceramic materials is their low fracture toughness, which usually does not exceed about 3.5 MPa·m$^{1/2}$(Lee et al., 2007; Suyama et al., 2003). Low values of K_{Ic} coefficient exclude these materials from numerous applications with dynamic loads, e.g. in machining processes.

There are various ways to improve the fracture toughness of ceramic materials. One of them involves obtaining a composite material by the introduction of the additional phases in the form of nano-, micro- or sub-micro-sized particles to the base material. Some papers indicate that nanosized structures have great potential to essentially improve the mechanical performance of ceramic materials even at high temperatures (Awaji et al., 2002; Derby, 1998; Kim et al., 2006; Niihara et al., 1999). Depending on the type of introduced particles, composites can take advantage of different strengthening mechanisms, such as the crack deflection, crack bridging, crack branching, crack bowing, crack pinning, microcracking, thermal residual stress toughening, transformation toughening and synergism toughening. For example, metallic particles are capable of plastic deformation, thus absorption of energy and bridging of a growing crack, resulting in increased strengthening (Fig. 1a) (Yeomans, 2008). On the other hand, hard ceramic particles, like borides or nitrides, can introduce a favorable stress state which can cause a toughening effect by crack deflection and crack bifurcation (Fig. 1b) (Xu, 2005). An addition of metal borides such as ZrB_2, TaB_2, NbB_2 or TiB_2, promote densification of SiC powder as well as improve hardness and other mechanical properties of the material as a whole (Tanaka et al., 2003).

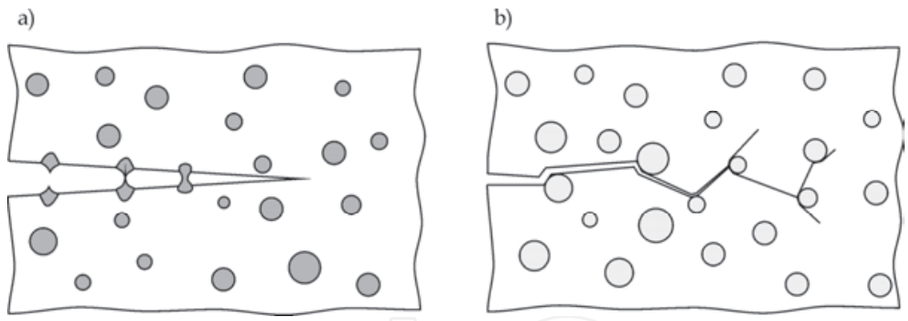

Fig. 1. Example of strengthening mechanisms which can occur in ceramic matrix composites with dispersed "soft" metallic or/and "hard" ceramic particles: a) crack bridging, b) crack deflection and crack bifurcation

The wide group of materials containing the silicon carbide are SiC/Si_3N_4 composites. In such materials predominant phase is silicon nitride, while SiC content does not usually exceed 30 vol.%. Silicon nitride has a lower hardness but a higher fracture toughness than silicon carbide. If SiC particles are uniformly dispersed in the Si_3N_4 ceramics, high strength can be obtained from room temperature to elevated temperature. It was reported that the strength of 1000 MPa at 1400°C is obtained in nano-composites having ultra-fine SiC particles added into the Si_3N_4 matrix. This improvement was mainly attributed to the suppression of a grain boundary sliding by intergranular SiC particles bonded directly with the Si_3N_4 grain in the atomic scale without any impurity phases (Hirano & Niihara, 1995; Yamada & Kamiya, 1999). SiC/Si_3N_4 composites have an ability to crack healing under high temperature and applied stress, to exhibit a significantly higher creep resistance and fracture

toughness compared to the monolithic materials. (Ando et al., 2002; Lojanová et al., 2010; Sajgalík et al., 2000; Takahashi et al., 2010).
The combination of the fair fracture toughness with high hardness, wear resistance and mechanical strength at elevated temperatures makes SiC/Si_3N_4 ceramics a promising material for cutting tools (Eblagon et al., 2007). Despite many studies on materials based on silicon carbide and silicon nitride, there is a lack of knowledge about the SiC/Si_3N_4 composites where the predominant phase is SiC. In the presented work, the materials contained from 0 to 100% of silicon carbide were investigated.

2. Description of experiment

The purpose of the presented experiment was to study the influence of High Pressure - High Temperature (HPHT) sintering on the phase composition, microstructure and selected properties of SiC/Si_3N_4 composites as well as to study the effect of the addition of third-phase particles selected from metals (Ti) or ceramics (TiB_2, cBN - cubic Boron Nitride) to the SiC – Si_3N_4 system. The main goal was to improve fracture toughness and wear resistance of the investigated materials.
The composites were manufactured and tested in two stages. The first stage consisted in sintering of materials having, in its initial composition, only SiC and/or Si_3N_4 powder(s). Samples sintered from nano-, sub-micro- and micropowders with various silicon carbide to silicon nitride ratios were investigated at this stage.
At the second stage the best SiC/Si_3N_4 composite manufactured at the first stage was subjected to modification, consisting of:

- use of various types of SiC and Si_3N_4 powders,
- addition of metallic phase in the form of Ti particles,
- addition of boride (TiB_2) phase,
- addition of superhard (cBN) phase.

All materials were sintered with the HPHT method. The parameters of sintering: time and temperature were chosen individually for each composition. The obtained samples were subjected to a series of studies, which included: phase composition and crystallite size analysis by X-ray diffraction, measurements of density by hydrostatic method and Young's modulus by the ultrasonic method, measurement of hardness and and fracture toughness using Vickers indentation as well as studies of tribological properties using the Ball-On-Disk method.

2.1 HPHT method of sintering

Pressure is a versatile tool in solid state physics, materials engineering and geological sciences. Under the influence of high pressure and temperature there are a lot of changes in physical, chemical and structural properties of materials (Eremets, 1996). It gives a possibility to generate of new, non-existent in nature phases, or phases which occur only in inaccessible places, such as the earth core (Manghnani et al., 1980). The use of pressure as a parameter in the study of materials was pioneered principally by Professor P. W. Bridgman, who for forty years investigated most of the elements and many other materials using diverse techniques (Bridgman, 1964). There are many design solutions to ensure High Pressure - High Temperature (HPHT) conditions for obtaining and examination of materials. Depending on the design assumptions, it is possible to achieve very high pressures, up to several hundred gigapascals, as in the case of Diamond Anvils Cell (DAC).

Such devices, due to their small size, are intended solely for laboratory investigations (XRD in-situ study, neutron diffraction etc.) (Piermarini, 2008). For the purposes of industrial and semi-industrial production of materials the most frequently the "Belt" or "Bridgman" type of equipment is used (Eremets, 1996; Hall, 1960; Khvostantsev et al., 2004). These apparatuses provide a relatively large working volume, the optimum pressure distribution and the possibility of achieving high temperatures.
In the toroidal type of Bridgman apparatus the quasi-hydrostatic compression of the material is achieved as a result of plastic deformation of the so called "gasket" (Fig. 2).

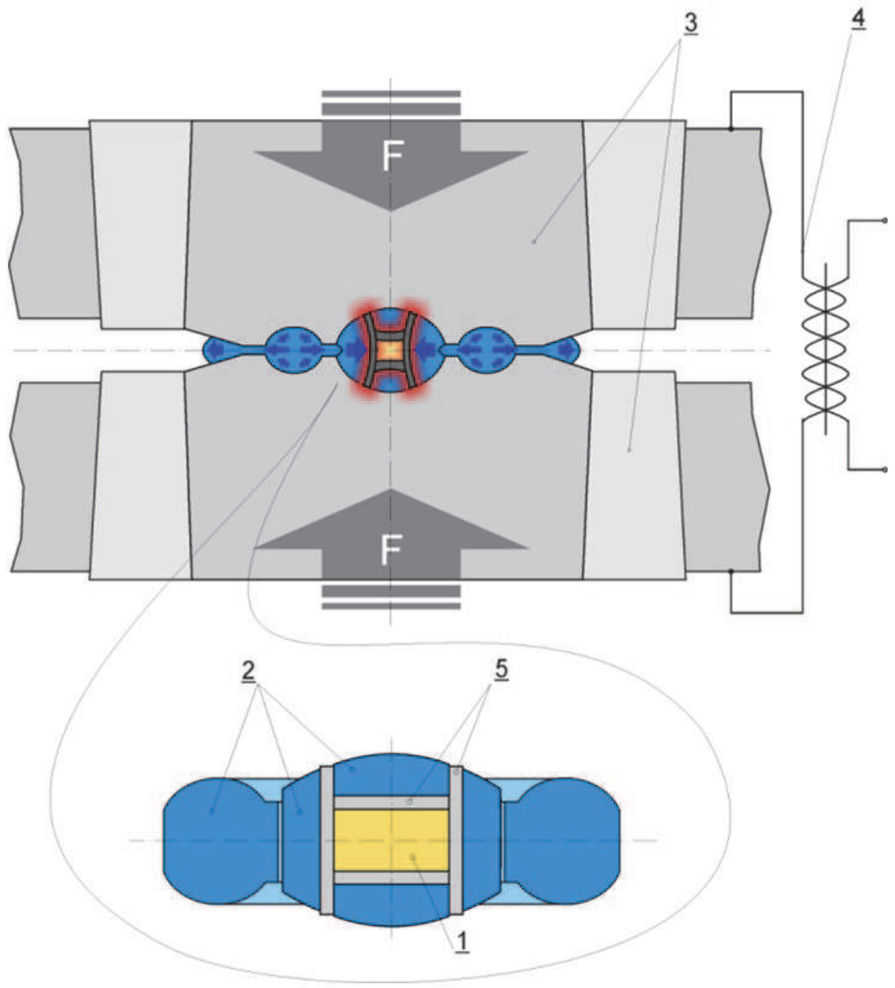

Fig. 2. Sintering process in a Bridgman-type HPHT system. Quasi-hydrostatic compression of the preliminary consolidated powders (sample - 1) is achieved as a result of plastic deformation of the gasket material (2) between anvils (3); electrical heating is provided by a high-power transformer (4) and graphite resistive heater (5)

Gaskets are made of special kinds of metamorphic rocks such as pyrophyllite, "lithographic stone" or catlinite (Filonenko & Zibrov, 2001; Prikhna, 2008). The toroidal chamber, depending on its volume (usually from od 0.3 do 1 cm^3), can generate pressures up to 12 GPa and temperature up to ~2500 °C. The presented system is used often for production of

synthetic diamonds and for sintering of wide range of superhard composites based on polycrystalline diamond (PCD) or polycrystalline cubic boron nitride (PcBN). Under the influence of a simultaneous action of pressure and temperature the sintering process occurs much faster than in the case of free sintering. A typical duration of sintering process with HPHT method is about 0.5 – 2 minutes (Fig. 3) while the free sintering requires several hours. Short duration of the process contributes to the grain growth limitation, which is essential in the case of sintering of nanopowdes. The materials obtained with HPHT method are characterized by almost a 100% level of densification, isotropy of properties and sometimes by a completely different phase composition in relation to the same free-sintered materials, due to the different thermodynamic conditions of the manufacturing process.

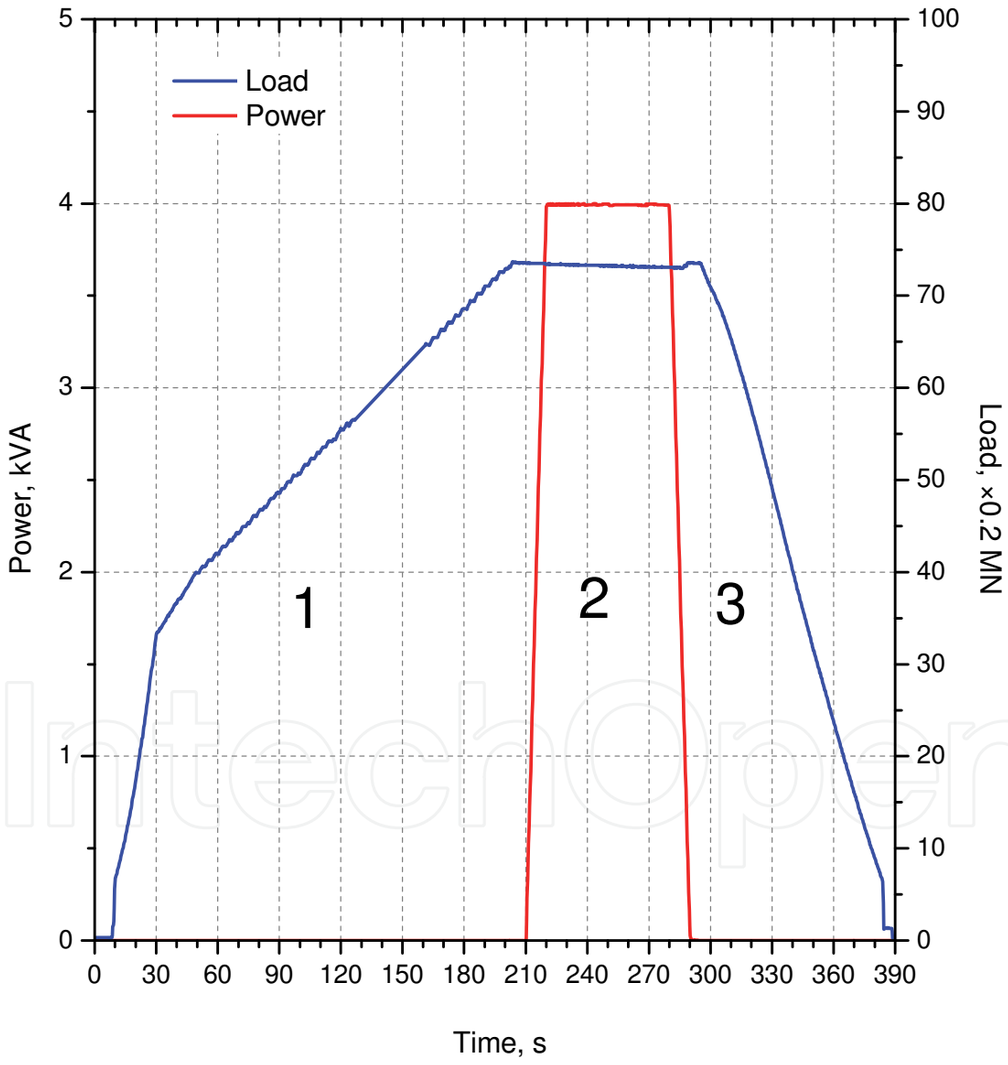

Fig. 3. Three stages of an example process of HPHT sintering: 1 – loading, 2 – sintering, 3 – unloading

2.2 Samples preparation

Powders used for the preparation of mixtures for sintering of SiC/Si_3N_4 materials are listed in Table 1.

Powder	Category	Particle size [μm]	Manufacturer	Description
SiC	nano	<5 nm	France	beta
SiC	sub-micro	0.1 – 1	Goodfellow, UK	alpha
SiC	micro	1.2	AGH, Poland	
Si_3N_4	nano	<20nm	Goodfellow, UK	amorphous
Si_3N_4	sub-micro	0.1 – 0.8	Goodfellow, UK	alpha
Si_3N_4	sub-micro	0.6	H.C. Starck, Germany	alpha>90%, M11-grade
Si_3N_4	micro	1 – 5	AEE, USA	alpha>85%
TiH_2	micro	<44	Fluka, Switzerland	
TiB_2	micro	2.5 – 3.5	H.C. Starck, Germany	F-grade
cBN	nano	0 – 0.1	Element6, South Africa	Micron+ABN, M0.10-grade
cBN	micro	3 – 6	Element6, South Africa	Micron+ABN, M36-grade

Table 1. Powders used for preparation of mixtures for sintering of SiC/Si_3N_4 materials

The following mixtures were prepared by mixing the appropriate powders (Table. 1) in an isopropanol environment using the Fritsch Pulverisette 6 planetary mill.

nano-SiC/Si_3N_4 materials

100 % SiC(nano)
100 % Si_3N_4(nano)
50 SiC(nano)/50 Si_3N_4(nano) – vol.%

sub-micro-SiC/Si_3N_4 materials

95 SiC(sub-micro)/5 Si_3N_4(sub-micro, Starck) – vol.%
70 SiC(sub-micro)/30 Si_3N_4(sub-micro, Starck) – vol.%
50 SiC(sub-micro)/50 Si_3N_4(sub-micro, Starck) – vol.%
100 % Si_3N_4(sub-micro, Starck)

micro-SiC/Si_3N_4 materials

70 SiC(micro)/30 Si_3N_4(micro) – vol.%
100 % Si_3N_4(micro)

70SiC/30Si_3N_4 composite (modification by using various SiC and Si_3N_4 powders)

70 SiC(sub-micro)/30 Si_3N_4(sub-micro, Starck) – vol.%
70 SiC(sub-micro)/30 Si_3N_4(sub-micro, Goodfellow) – vol.%
70 SiC(micro)/30 Si_3N_4(micro) – vol.%
70 SiC(sub-micro)/30 Si_3N_4(micro) – vol.%

70SiC/30Si_3N_4 composite + Ti (modification by addition of the third, metallic phase)

70 SiC(sub-micro)/30 Si_3N_4(sub-micro, Starck) + 8 vol.% Ti - from TiH_2(micro)

70SiC/30Si_3N_4 composite + TiB_2 (modification by addition of the third, boride phase)

70 SiC(sub-micro)/30 Si_3N_4(sub-micro, Starck) + 8 vol.% TiB_2(micro)
70 SiC(sub-micro)/30 Si_3N_4(sub-micro, Starck) + 30 vol.% TiB_2(micro)

70SiC/30Si_3N_4 composite + cBN (modification by addition of the third, nitride phase)
70 SiC(sub-micro)/30 Si_3N_4 (sub-micro, Starck) + 8 vol.% cBN(micro)
70 SiC(sub-micro)/30 Si_3N_4 (sub-micro, Goodfellow) + 8 vol.% cBN(nano)
70 SiC(sub-micro)/30 Si_3N_4 (sub-micro, Starck) + 30 vol.% cBN(micro)
After drying, the mixtures were preliminarily compressed into a disc of r 15 mm diameter and 5 mm height under pressure of ~200 MPa. The green bodies with the addition of TiH_2 were additionally annealed in a vacuum at a temperature of 800 °C for 1h in order to remove the hydrogen and obtain pure metallic titanium. The materials were obtained at high pressure (6 GPa) in the wide range of temperatures (430 – 2150 °C depending of composition) using a Bridgman-type toroidal apparatus (Fig. 2). The sintering temperatures were established experimentally for each material to obtain crack-free samples with the highest values of density and mechanical properties. The duration of the sintering process was 40s for nanopowders and 60 s for the others.
The sintered compacts were subsequently ground to remove remains of graphite after the technological process of sintering and to obtain the required quality and surface parallelism for Young's modulus determination. The samples provided for microscopic investigations and for mechanical tests were additionally polished using diamond slurries.

2.3 Investigation methods

Densities of the sintered samples were measured by the hydrostatic method. The uncertainty of the measurements was below 0.02 g/cm^3, which gave a relative error value of below 0.5 % (excluding measurements of small pieces of broken samples, where the error was up to 0.1 g/cm^3, due to their insufficient volume and mass).
Young's modulus of the samples obtained by HPHT sintering was measured by means of transmission velocity of ultrasonic waves through the sample, using a Panametrics Epoch III ultrasonic flaw detector. Calculations were carried out according to (Eq. 1):

$$E = \rho \cdot C_T^2 \frac{3C_L^2 - 4C_T^2}{C_L^2 - C_T^2} \tag{1}$$

where: E - Young's modulus, C_L - velocity of the longitudinal wave, C_T - velocity of the transversal wave, ρ - density of the material.
The velocities of transverse and longitudinal waves were determined as a ratio of sample thickness and relevant transition time. The accuracy of calculated Young's modulus (Eq. 1) was estimated to be below 2 %.
Hardness of sintered samples was determined by the Vickers method using a digital Vickers Hardness Tester (FUTURE-TECH FV-700). Five hardness measurements, with indentation loads of 2.94, 9.81 and 98.1 N, were carried out for each sample. Standard deviations of HV values were relatively high but usually no more than 5 % of the average values.
Indentation fracture toughness was calculated from the length of cracks which developed in a Vickers indentation test (with indentation load - 98.1 N) using Niihara's equation (Eq. 2):

$$\frac{K_{Ic}\varphi}{H\sqrt{a}}\left(\frac{H}{E\varphi}\right)^{\frac{2}{5}} = 0.129 \cdot \left(\frac{c}{a}\right)^{-\frac{3}{2}} \tag{2}$$

where: K_{Ic} - critical stress intensity factor, φ - constrain factor, H - Vickers hardness, E - Young's modulus, a - half of indent diagonal, c - length of crack.
Microstructural observations were carried out on the densified materials using a JEOL JXA-50A Scanning electron Microscope equipped with back scattering electron (BSE) imaging.
In the Ball-On-Disc tests, the coefficient of friction and the specific wear rate of the sintered samples in contact with Si_3N_4 ball were determined using a CETR UMT-2MT (USA) universal mechanical tester. In the Ball-On-Disc method, sliding contact is brought about by pushing a ball specimen onto a rotating disc specimen under a constant load (Fig. 4). The loading mechanism applied a controlled load F_n to the ball holder and the friction force was measured continuously during the test using an extensometer. For each test, a new ball was used or the ball was rotated so that a new surface was in contact with the disc. The ball and disc samples were washed in ethyl alcohol and dried.

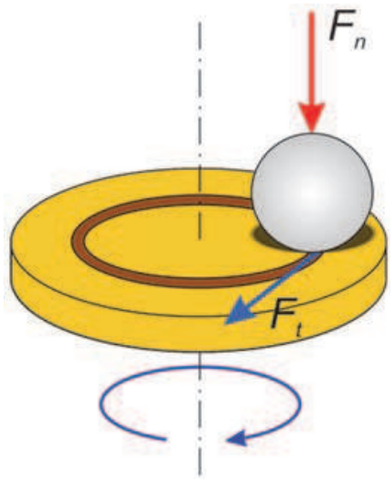

Fig. 4. Material pair for the Ball-On-Disc method: 1 – Si_3N_4 ball; 2 – sample (disc)

The size of the disc-shaped samples was ~13.5 in diameter and ~3.8 mm in height with the surfaces flatness and parallelism within 0.02 mm. The roughness of the tested surface was not more than 0.1 μm R_a. The following test conditions were established: ball diameter – 2 mm, applied load – 4 N, sliding speed – 0.1 m/s, diameter of the sliding circle – 2 ÷ 5 mm, sliding distance – 100 m, calculated duration of the test – 1000 s. The tests were carried out without lubricant at room temperature. Each test was repeated at least three times. Coefficient of friction was calculated from (Eq. 3):

$$\mu = \frac{F_f}{F_n} \tag{3}$$

where: μ – coefficient of friction, F_f – measured friction force, F_n – applied normal force.
After completing the test, according to ISO 20808:2004 E standard, the cross-sectional profile of the wear track at four places at intervals of 90° was measured using a contact stylus profilometer PRO500 (CETR, USA). Then the average cross-sectional area of the wear track was calculated. The volume of material removed was calculated as a product of cross-sectional area of the wear track and their circumference. Specific wear rate was calculated from (Eq. 4):

$$W_s = \frac{V}{F_n \cdot L} \tag{4}$$

where: W_s - specific wear rate, V – volume of removed material, L – sliding distance.

3. Materials sintered from nano-, sub-micro-, and micro-SiC/Si_3N_4 powders

A macroscopic view, phase composition and crystallite size of materials sintered from nanopowders under the pressure of 6 GPa at temperatures ranging from 430 to 1880 ° C in the period of time 40s are shown in Table 2.

Initial powders	β-SiC powder, 4.1 nm	Si_3N_4 amorphous powder, < 20 nm	Composite: 50 SiC/50 Si_3N_4 - vol.%
Temperature of sintering	Sintered material: appearance, phase composition, crystallite size		
430°C	-	 amorphous Si_3N_4	-
650°C	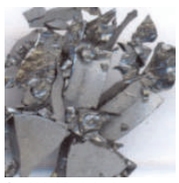 β-SiC (4.1 nm)	 amorphous Si_3N_4	 β-SiC (4.5 nm) + amorphous Si_3N_4
890°C	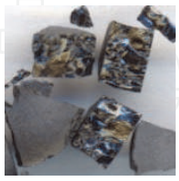 β-SiC (4.1 nm)	 amorphous Si_3N_4	 β-SiC (11.1 nm) + amorphous Si_3N_4
1170°C	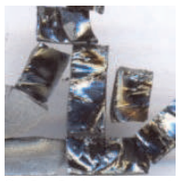 β-SiC (4.4 nm)	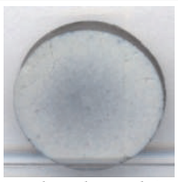 orthorhombic $Si_{1.8}Al_{0.2}O_{1.2}N_{1.8}$ (77)	 β-SiC (8.0 nm) + orthorhombic $Si_{1.8}Al_{0.2}O_{1.2}N_{1.8}$ (20.0 nm)

Initial powders	β-SiC powder, 4.1 nm	Si_3N_4 amorphous powder, < 20 nm	Composite: 50 SiC/50 Si_3N_4 - vol.%
Temperature of sintering	Sintered material: appearance, phase composition, crystallite size		
1450°C	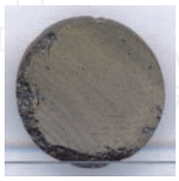 β-SiC (10.6 nm)	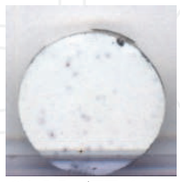 β-Si_3N_4 (77.4 nm)	 β-SiC (10.2 nm) + orthorhombic $Si_{1.8}Al_{0.2}O_{1.2}N_{1.8}$ (31.0 nm)
1880°C	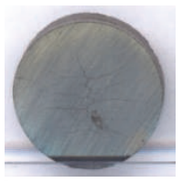 β-SiC (110 nm)	 β-Si_3N_4 (143 nm)	 β-SiC (51.8 nm) + β-Si_3N_4 (86.9 nm)

Table 2. A macroscopic view, phase composition and crystallite size of SiC/Si_3N_4 materials sintered from nanopowders under the pressure of 6 GPa at temperatures ranging from 430 to 1880 ° C in the period of time 40s

The initial crystallite size of sintered SiC nanopowder was about 4.1 nm and did not change until the sintering temperature of 1170 °C. At the sintering temperature of 1450°C crystallites reached an average size of 10.6 nm while at the maximum applied temperature (1880 °C) their size was 110 nm. This material showed no phase transformation. The sinters obtained at 1880 °C as well as the initial powder have the cubic structure of β-SiC phase.
Sintered Si_3N_4 powder remained amorphous until the temperature of 890 °C. At the temperature of 1170 °C a new phase crystallized. The X-ray diffraction pattern of this phase corresponds to the o'-sialon with orthorhombic structure and $Si_{1.8}Al_{0.2}O_{1.2}N_{1.8}$ stoichiometry. As evidenced by the chemical formula, this compound has a low content of aluminum with reference to silicon while the quantities of nitrogen and oxygen are comparable. It can be assumed that o'-sialon is a transition phase between the amorphous silicon nitride and a completely crystalline β-Si_3N_4 phase. O'-sialon was formed probably due to embedding a certain amount of oxygen and impurities adsorbed on the surface of powder to an atomic lattice of crystallizing silicon nitride. The crystallite size of this phase was estimated to around be 77 nm. The samples obtained at temperatures of 1450 and 1880 °C contain only β-Si_3N_4 phase with the crystallite size 77.4 and 143 nm respectively.
50 SiC/50 Si_3N_4 – vol.% nanocomposite was sintered at the same temperatures as silicon carbide powder without additions. The phase composition of sintered composites did not differ qualitatively from the sum of their components sintered separately. There was no formation of new phases in the reaction between silicon carbide and silicon nitride. Sintering of composites, especially at higher temperatures, leads to lower grain growth than it is in single-phase powders sintered separately. This indicates a favorable effect of inhibiting grain growth in the composite.

The comparison of physical-mechanical properties of nano-, sub-micro- and micro-SiC/Si_3N_4 materials sintered at different temperatures is presented in Fig. 5 and Table 3. Generally, nanocomposites are characterized by the lowest physical-mechanical properties of the three granulometric types of the investigated materials. Densities and Young's modulus values of the best nanostructured samples do not exceed 2.55 g/cm^3 and 135 GPa respectively. In most cases, nanostructured SiC/Si_3N_4 samples are characterized by a lot of cracks (see Table 2). Cracking of such ceramics occurs as a result of the presence in their structure of residual micro- and macro-stresses which overcome the strength of the produced material. The fine powder is characterized by a very large specific surface and high gas content in the sample due to the absorption process of the material particles. During heating, as a result of the increase in temperature, the volume of gases increases, which causes cracking or even permanent fragmentation of the sample. In order to prevent the cracking phenomena in the samples, various conditions of the sintering process were tested. Depending on composition, materials characterized by the highest level of densification and the best mechanical properties were obtained at different temperatures: 890 °C for pure Si_3N_4 and 1880 °C for 50 Si_3N_4/50 SiC – vol.% composite. Unfortunately, some of these samples had cracks as well. Different kinds of internal cracks, delamination and other defects of microstructure occurred in most of the nano-structured samples. These defects cause a scattering of caustic waves propagated through the material and, in consequence, the impossibility of Young's modulus measurements using ultrasonic probes (marked as **nm in Table 3).

Composites without cracks were obtained only from micro- and sub-micro-structured powders. Only for these composites hardness and fracture toughness were measured.

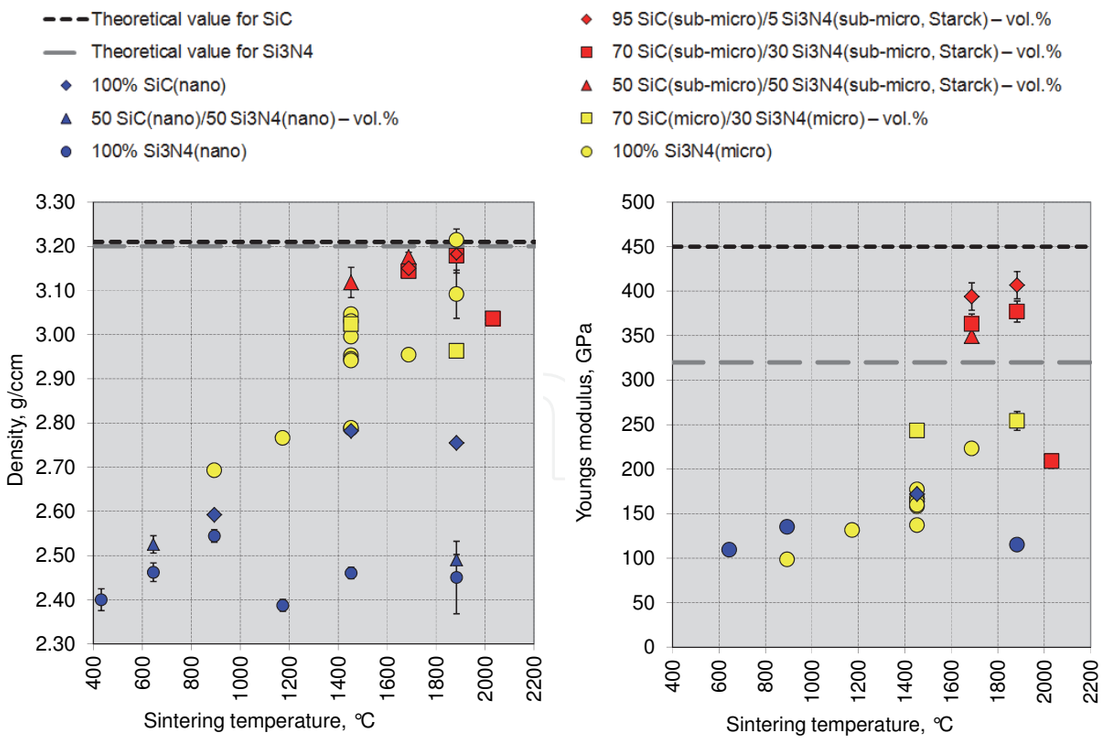

Fig. 5. Density and Young modulus of nano-, sub-micro-, and micro-SiC/Si_3N_4 materials sintered at different temperatures

Sample composition	Sintering temp. range	*Sintering temp. optimal for (properties) /descript-tion	Density		Youngs modulus		Poisson's ratio	Hardness			Fracture toughness
vol.%	°C	°C	g/ccm	% of theoretic	GPa	% of theoretic	-	$HV_{0.3}$	HV_1	HV_{10}	MPa $m^{1/2}$
nanomaterials (initial powders: β-SiC<5nm, amorphous Si_3N_4 <20nm) sintered at 6GPa for 40s											
100 SiC(nano)	650-1880	1450 /cracks	2.78	87	172	38	0.24	-	-	-	-
50 SiC(nano) /50 Si_3N_4(nano)	650-1880	1880 /small chipping	2.49	78	**nm	-	**nm	-	-	-	-
100 Si_3N_4(nano)	430-1880	890	2.54	80	135	42	0.24	-	-	-	-
sub-micro-structured materials (powders: α-SiC 0.1-1μm, α-Si_3N_4 0.6μm) sintered at 6GPa for 60s											
95 SiC(sub-micro) /5 Si_3N_4(sub-micro, Starck)	1690-2150	1880 /cracks	3.18	99	407	92	0.17	-	-	-	-
70 SiC(sub-micro) /30Si_3N_4(sub-micro, Starck)	1690-2030	*1690 (KIc)	3.14	98	363	87	0.19	2810	2630	2240	*5.6*
		1880 (ρ, E, HV)	*3.18*	*99*	*377*	*90*	*0.19*	*3130*	*2970*	*2400*	4.9
50 SiC(sub-micro) /50Si_3N_4(sub-micro, Starck)	1450-1880	1690	3.18	99	349	91	0.21	2700	2560	2140	5
100Si_3N_4(sub-micro, Starck)	1170-1690	/cracs	-	-	-	-	-	-	-	-	-
micro-structured materials (initial powders: SiC 1.2 μm, α-Si_3N_4 1-5 μm,) sintered at 6GPa for 60s											
70 SiC(micro) /30 Si_3N_4(micro)	1450-1880	1450 /small cracks	3.02	94	243	58	0.16	-	1880	1510	4.6
100 Si_3N_4(micro)	890-1880	*1450 (ρ)*	*3.03*	*95*	167	52	0.2	-	1250	1060	4.8
		1690 (E) /small chipping	2.95	92	*223*	*70*	0.22	-	-	-	-

Table 3. Physical-mechanical properties of selected nano-, sub-micro- and micro-SiC/Si_3N_4 materials sintered at optimal temperatures; *optimum temperature for selected properties, e.g. *1690 (K_{Ic})* - the best fracture toughness; **nm - non measurable with ultrasonic method

	Si_3N_4 based ceramics				SiC based ceramics			Sub-micro-70SiC/30Si_3N_4 composites (this work)	
	StarCeram N 7000 H.C. Starck	StarCeram N 8000 H.C. Starck	EKatherm Ceradyne	Ceralloy 147-A Ceradyne	StarCeram S H.C. Starck	Hexoloy SA Saint Gobain	Ceralloy 146-S5 Ceradyne		
Density, g/ccm	>3.22	>3.23	>3.24	3.18	3.10	3.10	3.20	**3.14**	**3.18**
Young's modulus, GPa	290	310	310	310	395	410	430	**363**	**377**
Vickers hardness, HV	1500	1520	1450 (300g)	1650 (300g)	2500	2800 (100g Konopp)	2600 (300g)	**2812 (300g)**	**3132 (300g)**
Fracture toughness, MPa·$m^{1/2}$	6.7	6.0	7.0	4.5	3.0	4.6	4.3	**5.6**	**4.9**

Table 4. Comparison of commercial advanced SiC/Si_3N_4-based ceramics[1] with sub-micro-structured 70 SiC/30 Si_3N_4 – vol.% composites obtained by HPHT sintering

The composites obtained from submicron powders are characterized by the best properties. Density and Young's modulus of the best 70 SiC/30 Si_3N_4 – vol.% compacts sintered at 1880 °C were 3.18 g/cm^3 and 377 GPa respectively (over 99% and 90% of the theoretical values). This material is also characterized by the highest hardness (HV1 ~3000) and relatively good fracture toughness (4.9 MPa·$m^{1/2}$). The same material sintered at a lower temperature (1690 °C) has slightly lower values of density (3.14 g/cm^3), Young's modulus (363 GPa) and hardness (HV1 2626) but higher fracture toughness (5.6 MPa·$m^{1/2}$) - Table 3. HPHT sintered sub-micro-70 SiC/30 Si_3N_4 – vol.% composites have a better combination of mechanical properties than comparable commercial materials (Table 4).

The composites obtained from the micro-sized powders have their properties intermediate between the nano- and sub-micro-structured materials. Even though the best micro-SiC/Si_3N_4 samples are crack free and have fairly good density (>94% of theoretical values) and indentation fracture toughness (4.6 – 4.8 MPa·$m^{1/2}$), their Young's modulus and hardness are much lower than for the sub-micro-structured samples. The insufficient mechanical properties of microstructured Si_3N_4–SiC materials can be attributed not only to grain size but also to specific properties of the initial powder resulting from their production method (e.g. shape of the grains, impurities, oxidation etc.). The choice of suitable initial powders for the given method of sintering is the critical factor in achieving good quality of ceramics.

[1] Data from: H.C. Starck Ceramics GmbH& Co. KG, Ceradyne Inc. and Saint – Gobain Advanced Ceramics – commercial data sheets)

For all the investigated samples, independently of their grain size, a strong influence of indentation load on hardness values can be observed. Increasing the indentation load causes a decrease in hardness values (Table 3).

4. Modifications of 70 SiC/30 Si_3N_4 composite

Density and Young's modulus of various 70 SiC/30 Si_3N_4 – vol.% composites sintered at different temperatures with and without additions of Ti, TiB_2 and cBN phases are presented in Figs 6-11 and in Table 5.

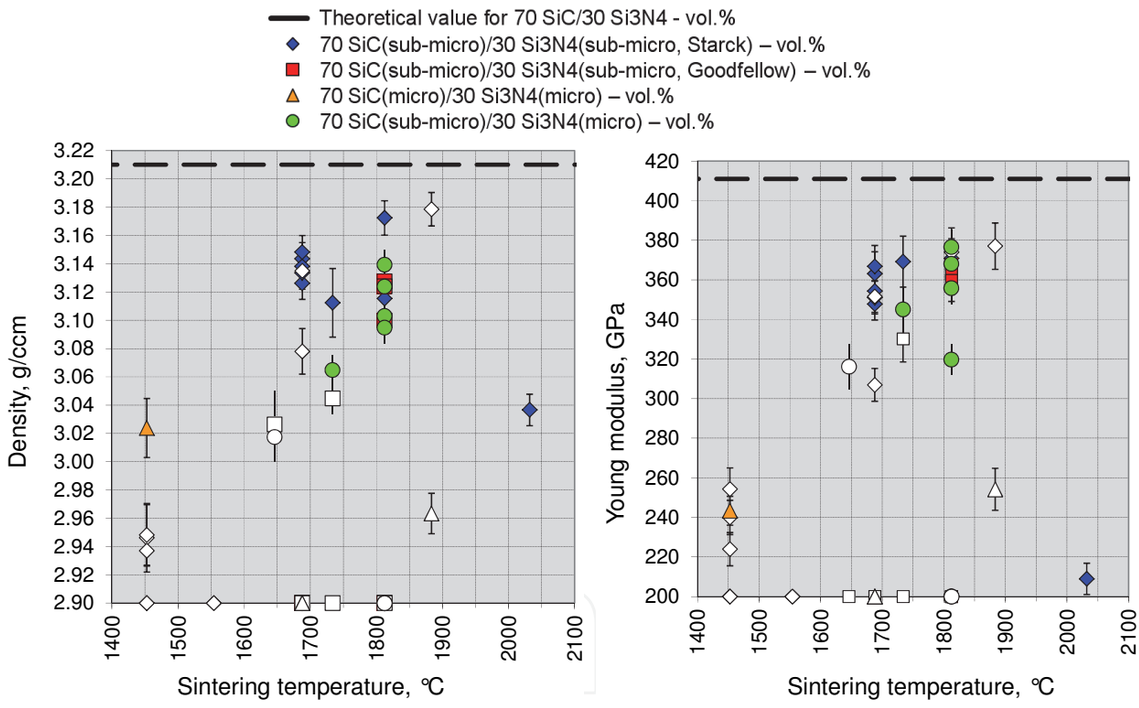

Fig. 6. Density and Young's modulus of various kinds of 70 SiC/30 Si_3N_4 – vol.% composites sintered at different temperatures. Colored symbols – samples without cracks; white symbols – samples with cracks; white symbols placed on temperature axis – broken samples

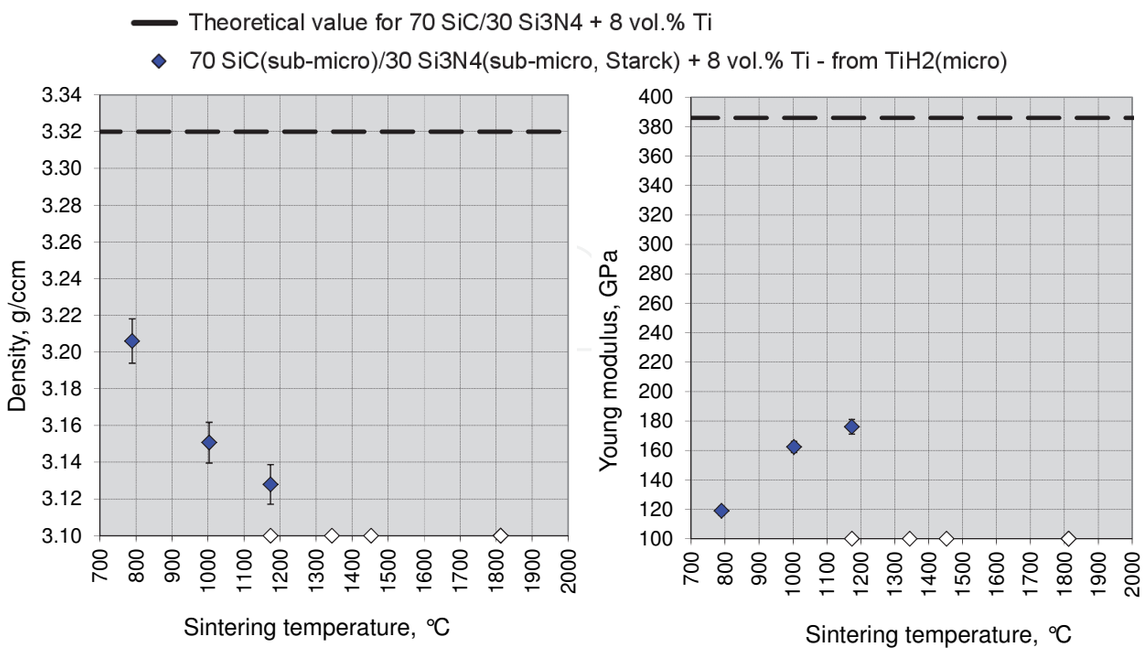

Fig. 7. Density and Young's modulus of 70 SiC/30 Si_3N_4 + 8 vol.% Ti composites sintered at different temperatures. Dark symbols – samples without cracks; white symbols – samples with cracks; white symbols placed on temperature axis – broken samples

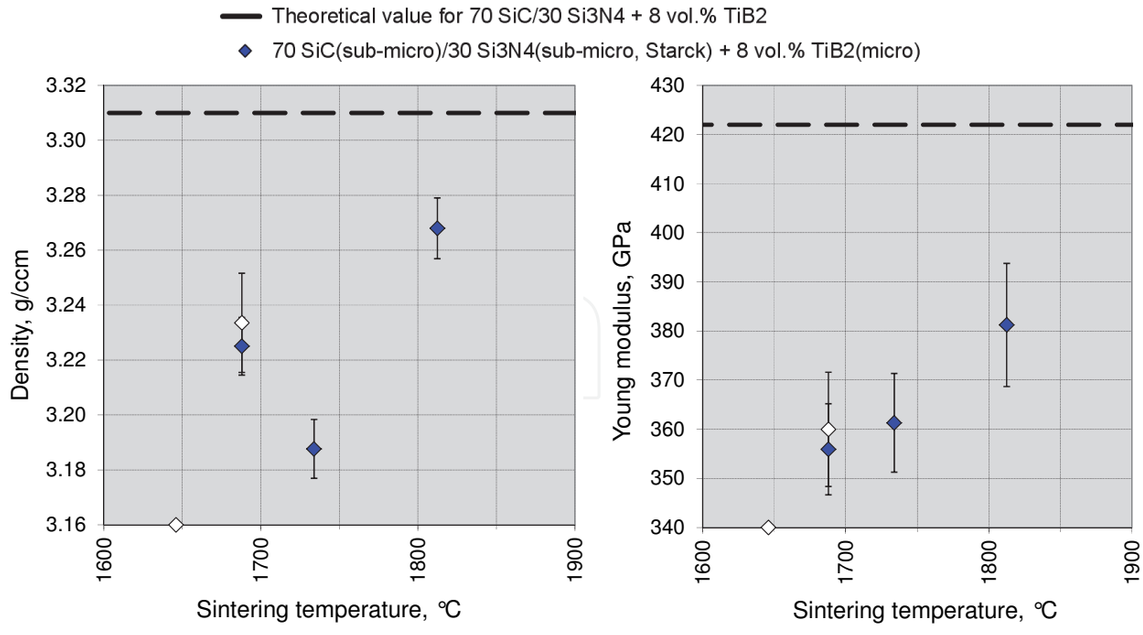

Fig. 8. Density and Young's modulus of 70 SiC/30 Si_3N_4 + 8 vol.% TiB_2 composites sintered at different temperatures. Dark symbols – samples without cracks; white symbols – samples with cracks; white symbols placed on temperature axis – broken samples

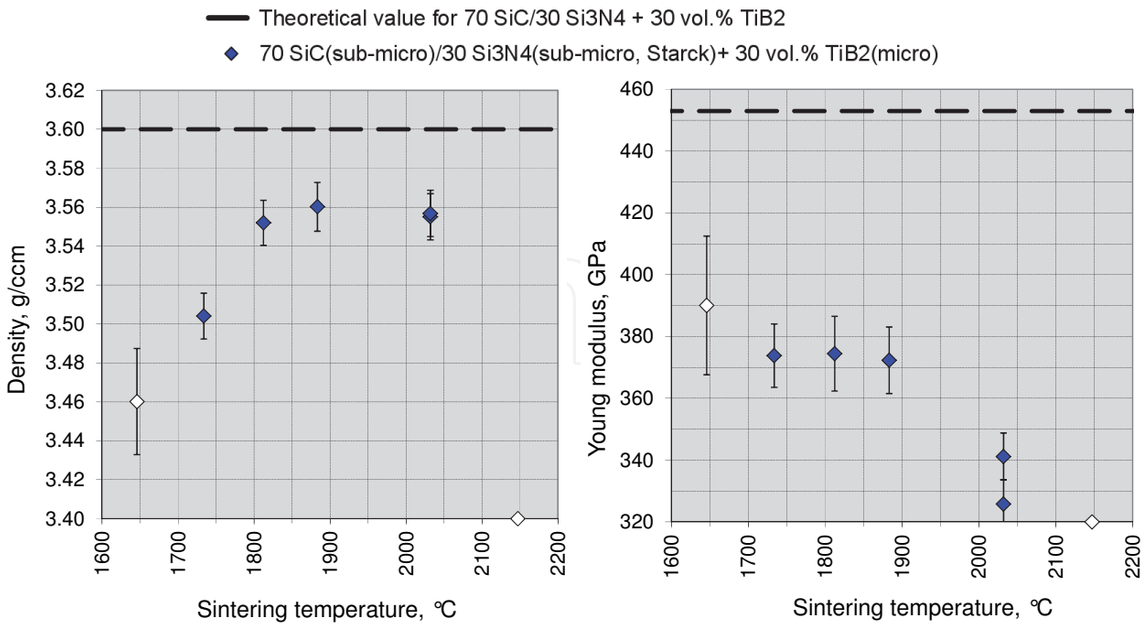

Fig. 9. Density and Young's modulus of 70 SiC/30 Si_3N_4 + 30 vol.% TiB_2 composites sintered at different temperatures. Dark symbols – samples without cracks; white symbols – samples with cracks; white symbols placed on temperature axis – broken samples

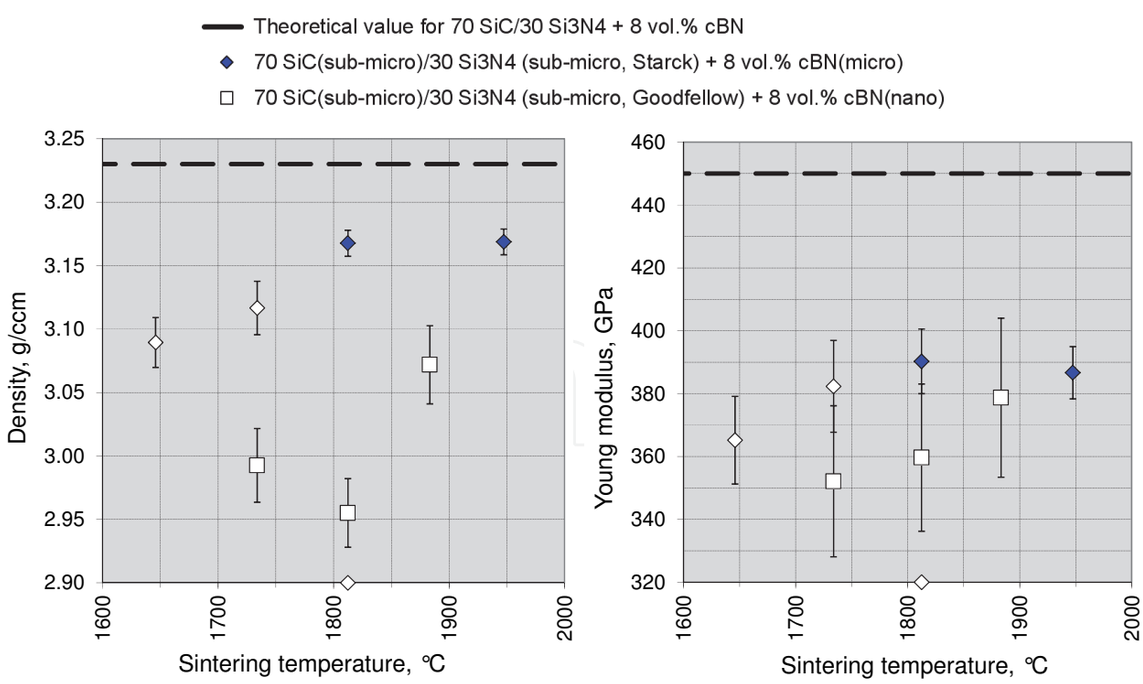

Fig. 10. Density and Young's modulus of 70 SiC/30 Si_3N_4 + 8 vol.% cBN composites sintered at different temperaturesDark symbols – samples without cracks; white symbols – samples with cracks; white symbols placed on temperature axis – broken samples

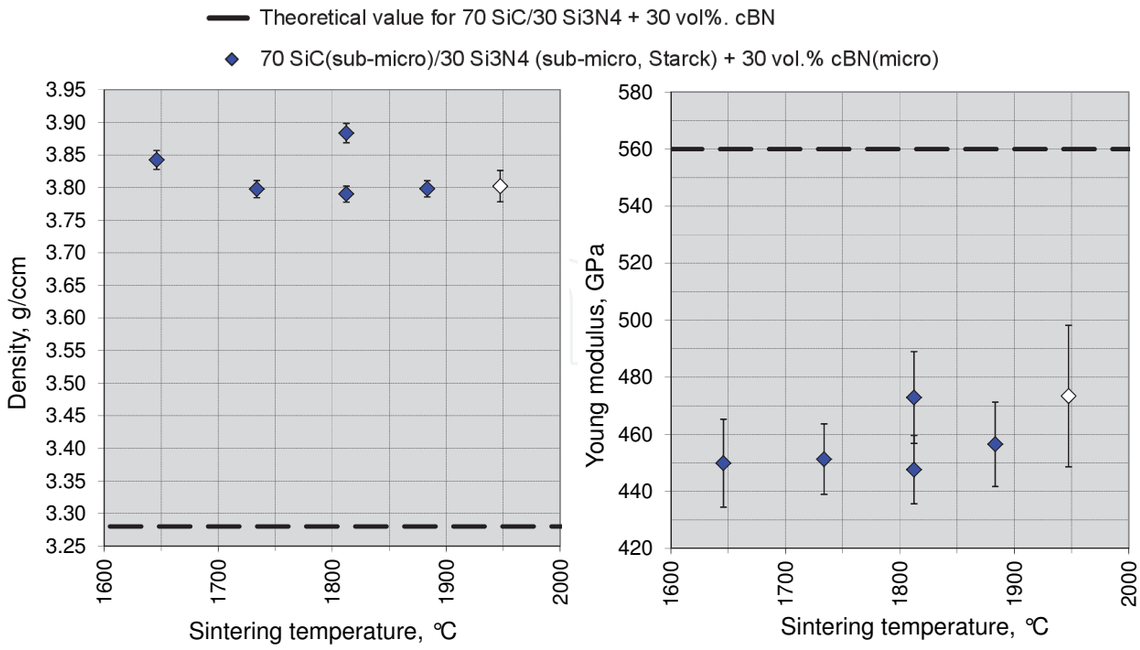

Fig. 11. Density and Young's modulus of 70 SiC/30 Si_3N_4 + 30 vol.% cBN composites sintered at different temperatures. Dark symbols – samples without cracks; white symbols – samples with cracks

Among the composites sintered without additional phases, the highest degree of densification and best mechanical properties were demonstrated by composite obtained from submicron powders 70 SiC(sub-micro)/30 Si_3N_4(sub-micro, Starck) – vol%. (Fig. 6 and Table 5). This composite was selected for modification by the addition of the third phase particles.

The modification of the 70 SiC/30 Si_3N_4 composite by the addition of Ti was not successful. The samples with the addition of 8 vol.% Ti introduced in the form of TiH_2, sintered at low temperatures, were characterized by a very low Young's modulus, whilst all the samples sintered at temperatures above ~1200 °C were cracked. A decrease in density was observed with increasing sintering temperature, whilst Young's modulus showed an upward trend (Fig. 7).

The composites with the addition of TiB_2 were characterized by a high degree of densification, a high Young's modulus and improved K_{Ic} as compared to the unmodified composite. No improvement in hardness was observed (Table 5). In the case of 70 SiC/30 Si_3N_4 material with the addition of 8 vol.% TiB_2, there is some increase in density and Young's modulus with increasing temperature (Fig. 8). Composite with the addition of 30 vol.% TiB_2, shows an increase in density with sintering temperature up to a maximum value, and then its stabilization. A further increase of the sintering temperature results in cracking of the samples (Fig. 9).

The composites modified by the addition of 8 vol.% cBN micropowder have better properties than the composites with TiB_2 but a tendency to cracking of this material is noticeable. The use of nano-cBN particles as a modifier causes the deterioration of the properties and cracking of samples (Fig. 10). The composites modified by the addition of 30 vol.% cBN micropowder, showed the best mechanical properties (Fig. 11 and Table 5).

Sample composition	Sintering temp. range	Sintering temp. optimal for (properties) / description	Density		Youngs modulus		Poisson's ratio	Hardness		Fracture toughness
vol.%	°C	°C	g/ccm	% of theoretic	GPa	% of theoretic	GPa	HV_1	HV_{10}	MPa $m^{1/2}$
70SiC/30Si_3N_4 composite										
70 SiC(sub-micro)/ 30 Si_3N_4(sub-micro, Starck)	1450-2030	**1880 (ρ, E, HV)*	*3.18*	*99*	*377*	*92*	*0.19*	*2970*	*2400*	4.9
		**1690 (K_{Ic})*	3.14	98	363	87	0.19	2630	2240	*5.6*
70 SiC(sub-micro)/ 30 Si_3N_4(sub-micro, oodfellow)	1650-1810	1810 /cracks	3.13	97	368	89	0.20	2772	2268	5.7
70 SiC(micro)/ 30 Si_3N_4(micro)	1450-1880	1450 /small cracks	3.02	94	243	58	0.16	1880	1510	4.6
70 SiC(sub-micro)/ 30 Si_3N_4(micro)	1650-1810	**1810 (ρ, E, HV)*	*3.10*	*97*	*368*	*90*	*0.20*	*2748*	*2392*	5.6
		**1730 (K_{Ic}) /small cracks*	3.06	95	345	84	0.20	2576	2278	*6.0*
70SiC/30Si_3N_4 composite + Ti										
70 SiC(sub-micro)/ 30 Si_3N_4(sub-micro, Starck) + 8 Ti – from TiH_2 (micro)	790-1810	**790 (ρ)*	*3.21*	*97*	119	31	0.13	-	-	-
		**1170 (E)*	3.13	94	*176*	*46*	0.10	-	-	-
70SiC/30Si_3N_4 composite + TiB_2										
70 SiC(sub-micro)/ 30 Si_3N_4(sub-micro, Starck) + 8 TiB_2(micro)	1650-1810	**1810 (ρ, E)*	*3.27*	*99*	*381*	*90*	0.20	2488	2364	4.2
		**1690 (K_{Ic})*	3.23	97	356	84	0.18	2526	2324	*6.1*
70 SiC(sub-micro)/ 30 Si_3N_4(sub-micro, Starck) + 30 TiB_2(micro)	1650-2150	**1810 (ρ, HV)*	*3.55*	*99*	374	83	0.17	*2564*	*2318*	5.8
		**1730 (K_{Ic})*	3.50	97	374	83	0.17	2390	2260	*6.4*
70SiC/30Si_3N_4 composite + cBN										
70 SiC(sub-micro)/ 30 Si_3N_4(sub-micro, Starck) + 8cBN(micro)	1650-1950	1950 /cracks	3.17	98	387	86	0.19	2850	2408	6.4
70 SiC(sub-micro)/ 30 Si_3N_4(sub-micro, Goodfellow) + 8cBN(nano)	1730-1880	1880 /cracks	3.07	95	379	84	0.17	-	-	-
70 SiC(sub-micro)/ 30 Si_3N_4(sub-micro, Starck) + 30cBN(micro)	1650-1950	**1810 (ρ, E) /cracks*	*3.88*	*118*	*473*	*84*	0.18	3038	2612	7.4
		**1880 (HV, K_{Ic})*	3.80	116	457	82	0.18	*3190*	*2790*	*7.5*

Table 5. Physical-mechanical properties of the best samples selected from different modifications of 70 SiC/30 Si_3N_4 composites; *optimum temperature for selected properties, e.g. *1690 (K_{Ic})* - the best value of fracture toughness

SEM microstructures of 70 SiC/30 Si_3N_4 with and without the addition of TiB_2 and cBN are presented in Fig. 12. The microstructures of the investigated samples are compact and dense, with the ingredients uniformly distributed in the volume of the composite. This demonstrates successful blending, using a planetary mill; EDS analysis, however, showed a

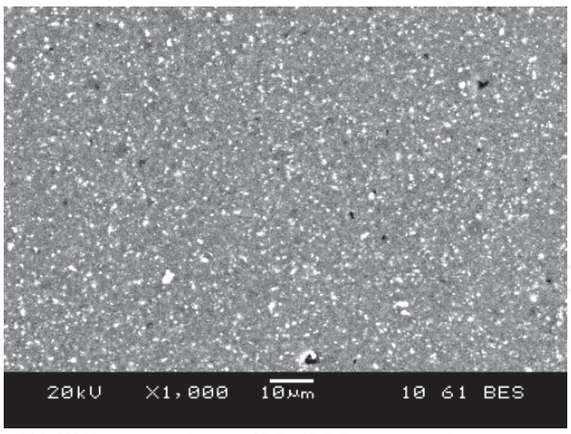

70 SiC(sub-micro)/30 Si_3N_4(sub-micro, Starck) – vol.%

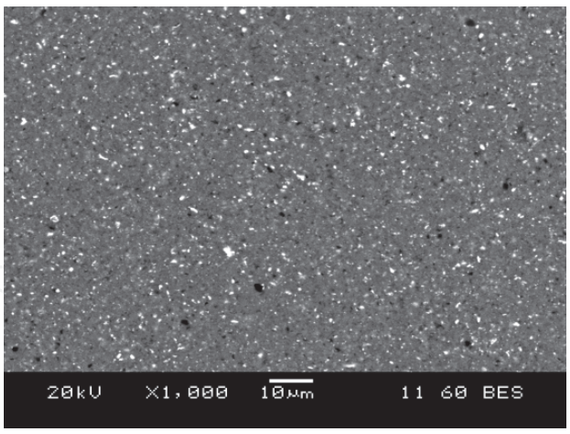

70 SiC(micro)/30 Si_3N_4(micro) – vol.%

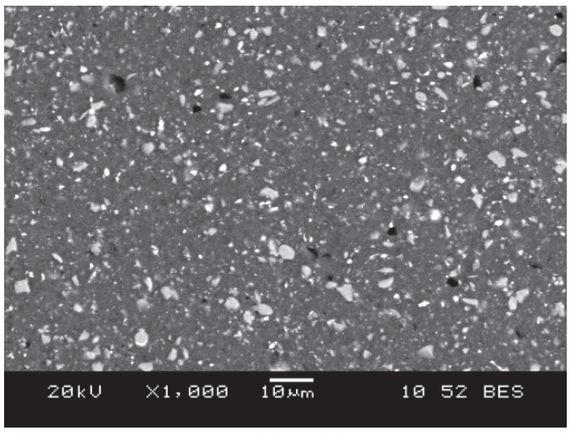

70 SiC(sub-micro)/30 Si_3N_4(sub-micro, Starck) + 8 vol.% TiB_2(micro)

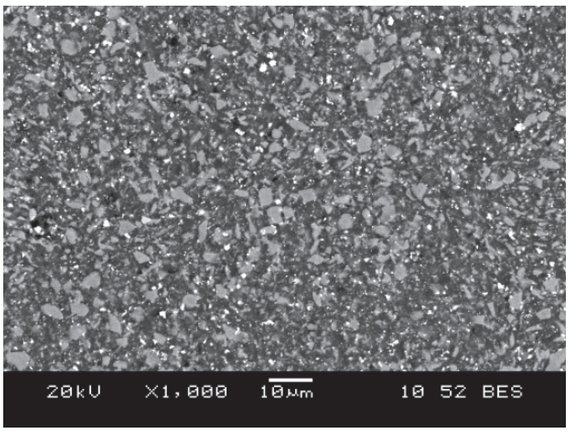

70 SiC(sub-micro)/30 Si_3N_4(sub-micro, Starck) + 30 vol.%TiB_2(micro)

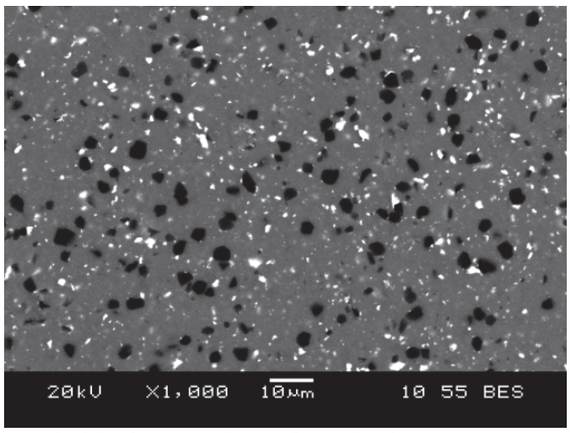

70 SiC(sub-micro)/30 Si_3N_4(sub-micro, Starck) + 8 vol.% cBN(micro)

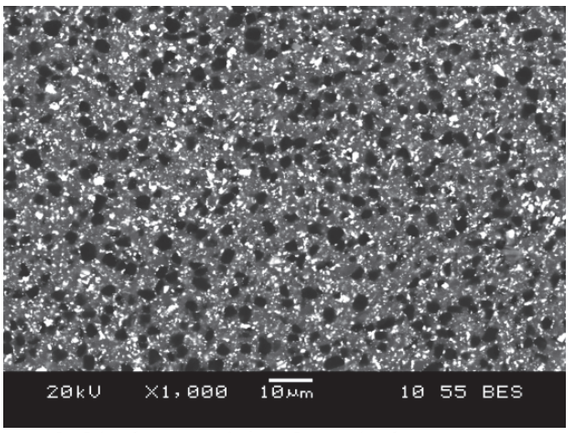

70 SiC(sub-micro)/30 Si_3N_4(sub-micro, Starck) + 30 vol.% cBN(micro)

Fig. 12. SEM microstructures of selected 70 SiC/30 Si_3N_4 composites with and without the addition of TiB_2 and cBN

high content of tungsten carbide and zirconium dioxide from the vessel and grinding media used to prepare the mixtures (white areas visible in the microstructures - Fig. 12). The highest quantity of WC was admixed to composite containing 30% of cBN super-abrasive powder. WC has density of 15.7 g/cm^3. It explains too high value (118%) of relative density of 70 SiC/30 Si_3N_4 + 30vol.% cBN composite.

An example of a crack which developed in a Vickers indentation test in the composite modified by addition 30% of cBN is presented in Fig. 13. In this material the mixed mode of crack propagation can be observed. Some parts of fracture are of an intra-crystalline character (indicated as **1** in Fig. 13) while some are inter-crystalline (indicated as **2** in Fig. 13). In both cases the change of direction of crack propagation is visible. A similar effect can be observed in the composites modified by the TiB_2 phase. This indicates that the crack deflection mechanism influences on toughening of composites modified by ceramic particles.

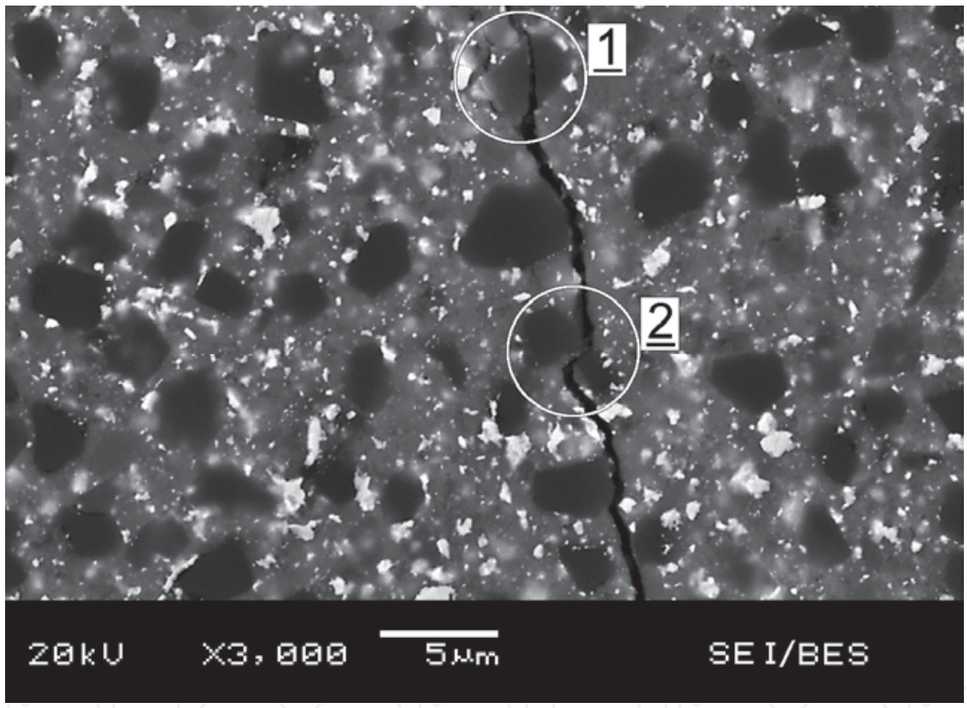

Fig. 13. SEM microstructure of 70 SiC/30 Si_3N_4 composite modified by addition of 30 vol.% cBN phase (the darkest areas). Mixed mode of crack propagation visible: 1) crack propagates through the cBN grains, 2) crack propagates around the cBN grains

High-quality composites, characterized by the homogeneous microstructure, without cracks (formed during the third stage of HPHT sintering process - cooling and releasing of the pressure) and high values of Young's modulus, hardness and fracture toughness were subjected to the tribological tests. The above criteria were fulfilled for following materials:
70 SiC(sub-micro)/30 Si_3N_4(sub-micro, Starck) – vol.%,
70 SiC(sub-micro)/30 Si_3N_4(micro) – vol.%,
70 SiC(sub-micro)/30 Si_3N_4(sub-micro, Starck) + 8 vol.% TiB_2(micro),
70 SiC(sub-micro)/30 Si_3N_4(sub-micro, Starck)+ 30 vol.% TiB_2(micro),
70 SiC(sub-micro)/30 Si_3N_4 (sub-micro, Starck) + 30 vol.% cBN(micro).

Additionally, for comparison, the commercial Si_3N_4 based cutting tool material (ISCAR, IS9-grade) was also tested. The mean curves of friction coefficient for investigated materials in a sliding contact with the Si_3N_4 ball are presented in Fig. 14. A comparison of the specific wear rate determined by the wear tracks measurement is presented in Fig. 15.

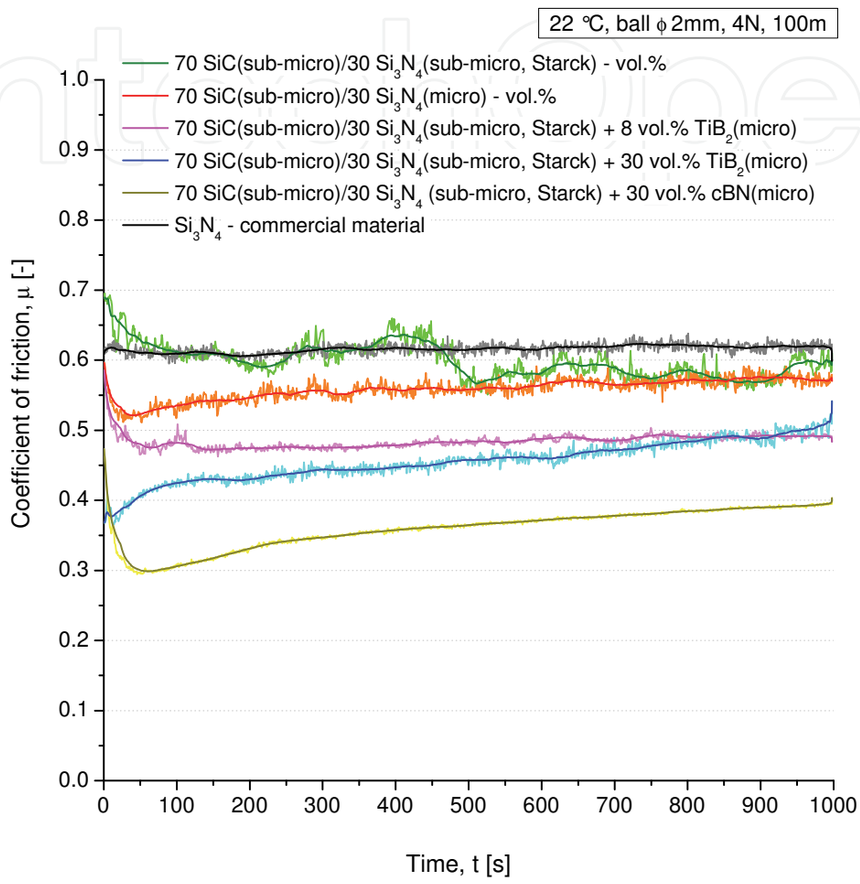

Fig. 14. Coefficient of friction of selected 70 SiC/30 Si_3N_4 – vol.% composites with and without the addition of TiB_2 and cBN

70 SiC/30 Si_3N_4 composites, sintered without additional phases, as well as the commercial material had the highest coefficients of friction. Average values of the friction coefficient for 70 SiC(sub-micro)/30 Si_3N_4(sub-micro, Starck), 70 SiC(sub-micro)/30 Si_3N_4(micro) composites and for commercial Si_3N_4 based cutting tool material were 0.60, 0.56 and 0.62 respectively. The composites modified by the addition of a TiB_2 phase were characterized by intermediate values of the friction coefficient. Average values of the friction coefficient for 70 SiC(sub-micro)/30 Si_3N_4(sub-micro, Starck) + 8 vol.% TiB_2(micro) and 70 SiC(sub-micro)/30 Si_3N_4(sub-micro, Starck) + 30 vol.% TiB_2(micro) materials were 0.48 and 0.46 respectively. The composite with the addition of 30% cBN was characterized by the lowest average coefficient of friction, at only 0.36. High coefficients of friction generate thermal stress, which is detrimental to the wear behavior of materials. Hard ceramic bodies – possessing high fracture toughness and low coefficients of friction – used in mechanical

systems that involve high loads, velocities and temperatures, will reduce costs and be less harmful to the environment.

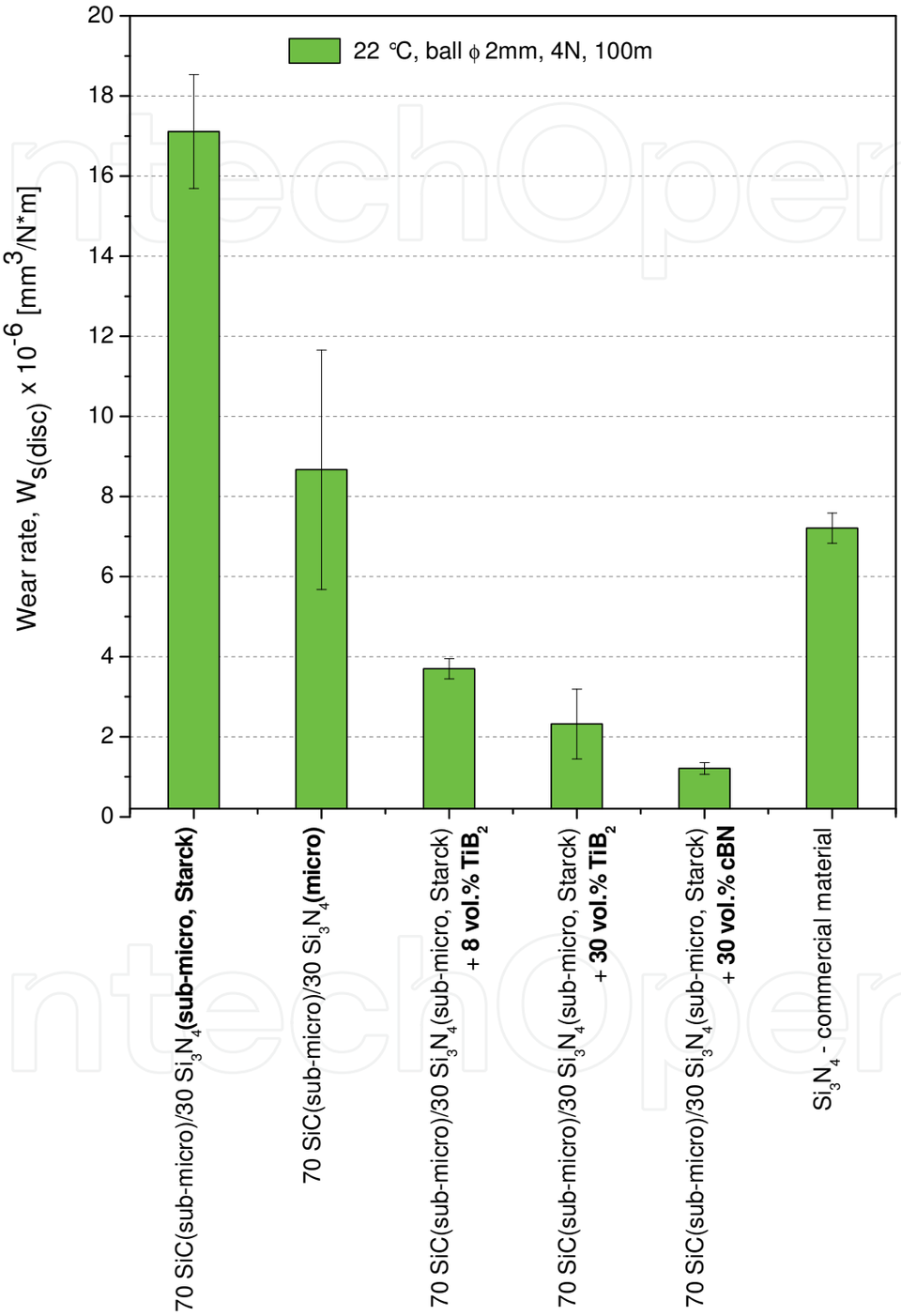

Fig. 15. Wear rate of selected 70 SiC/30 Si_3N_4 – vol.% composites with and without the addition of TiB_2 and cBN

Specific wear rates of investigated materials, in most cases, show a similar trend to the trends exhibited by their coefficients of friction. Only 70 SiC/30 Si_3N_4 composites without addition of third phase and commercial material show some deviations from this trend. 70 SiC(sub-micro)/30 Si_3N_4(sub-micro, Starck) composite is the least wear resistant. Their specific wear rate reached value of 17.1×10^{-6} $mm^3/N \cdot m$. Subsequently 70 SiC(sub-micro)/30 Si_3N_4(micro) and commercial material are classified. Their specific wear rates are 8.7×10^{-6} and 7.2×10^{-6} $mm^3/N \cdot m$ respectively. Significantly better are composites modified by addition of TiB_2 particels. The specific wear rate of 70 SiC(sub-micro)/30 Si_3N_4(sub-micro, Starck) + 8 vol.% TiB_2(micro) and 70 SiC(sub-micro)/30 Si_3N_4(sub-micro, Starck)+ 30 vol.% TiB_2(micro) samples equal 3.7×10^{-6} and 2.3×10^{-6} $mm^3/N \cdot m$ respectively. The highest wear resistant is exhibited by 70 SiC(sub-micro)/30 Si_3N_4 (sub-micro, Starck) + 30 vol.% cBN(micro) composite with its specific wear rate value equals only 1.2×10^{-6} $mm^3/N \cdot m$.

5. Conclusions

The performed research proves that the HPHT sintering is a method of the future for compacting SiC/Si_3N_4 nanopowders, due to the short time of the process amounting to 40 seconds that permits the grain growth limitations. The obtained compacts were characterized by the crystallites sizes of 4 to 143 nm, depending on the sintering parameters. SiC and SiC/Si_3N_4 samples sintered from nanopowders are characterized by the presence of cracks. Cracking of such ceramics occurs as a result of residual micro- and macro-stresses in their structure which overcome the strength of the produced material. The fine powder is characterized by a very large specific surface and high gas content in the sample due to the absorption process of the material particles. During heating, as a result of the increase in temperature, the volume of gases increases, which causes cracking or even permanent fragmentation of the sample. The research regarding the mechanical properties of SiC/Si_3N_4 composites indicates that materials obtained from submicron powders display the best properties. Density and Young's modulus of the best 70 SiC/30 Si_3N_4 – vol.% compacts, sintered at 1880 °C, were 3.18 g/cm^3 (over 99% the theoretical values) and 377 GPa respectively. This material is also characterized by the highest hardness (HV1 ~3000) and relatively good fracture toughness (4.9 $MPa \cdot m^{1/2}$). The same material sintered at a lower temperature (1690 °C) has slightly lower values of density (3.14 g/cm^3), Young's modulus (363 GPa) and hardness (HV1 2626) but higher fracture toughness (5.6 $MPa \cdot m^{1/2}$). HPHT sintered sub-micro-70 SiC/30 Si_3N_4 – vol.% composites have a better combination of mechanical properties than comparable commercial materials.

The research concerning mmodification of sub-micro-70 SiC/30 Si_3N_4 – vol.% composites proves that the addition of the third phase in the form of TiB_2 or cBN particles contribute to their further improvement. Composites modified by the addition of 30vol.% cBN micropowder are characterized by the best combination of Young's modulus, hardness, fracture toughness, coefficient of friction and the specific wear rate. Such properties predispose 70 SiC/30 Si_3N_4 + 30vol.% cBN composites to various advanced engineering applications including their use for wear parts and cutting tools.

6. Acknowledgments

This study was carried out within the framework of the project funded by the Polish Ministry of Science and Higher Education (Project number: DPN/N111/BIALORUS/2009).

The author would like to thank Prof. M. Bućko from AGH University of Science and Technology in Krakow for XRD analysis. The author would also like to thank his colleagues from The Institute of Advanced Manufacturing Technology in Krakow for Vickers's indentation tests and for SEM studies. Finally, the author would like to thank his supervisor Prof. L. Jaworska for her optimism and valuable advice throughout this research.

7. References

Ando, K.; Houjyou, K.; Chu, M.C.; Takeshita, S.; Takahashi, K.; Sakamoto, S. & Sato, S. (August 2002). Crack-healing behavior of Si_3N_4/SiC ceramics under stress and fatigue strength at the temperature of healing (1000 °C). *Journal of the European Ceramic Society*, Vol. 22, No. 8, pp. 1339 - 1346, ISSN 0955-2219

Awaji, H.; Choi, S. & Yagi, E. (July 2002). Mechanisms of toughening and strengthening in ceramic-based nanocomposites. *Mechanics of Materials*, Vol. 34, No. 7, pp. 411 - 422, ISSN 0167-6636

Bridgman, P.W. (1964). *Collected Experimental Papers*, Harvard University Press, ISBN 0674137507, Cambridge, Massachusetts, USA

Derby, B. (October 1998). Ceramic nanocomposites: mechanical properties. *Current Opinion in Solid State and Materials Science*, Vol. 3, No. 5, pp. 490-495, ISSN 1359-0286

Eblagon, F.; Ehrle, B.; Graule, T. & Kuebler, J. (2007). Development of silicon nitride/silicon carbide composites for wood-cutting tools. *Journal of the European Ceramic Society*, Vol. 27, No. 1, pp. 419 - 428, ISSN 0955-2219

Eremets, M.I. (1996). *High pressure Experimental Methods*, Oxford University Press, ISBN 0-19-856269-1, New York, USA

Filonenko, V.P. & Zibrov, I.P. (September 2001). High-Pressure Phase Transitions of M_2O_5(M = V, Nb, Ta) and Thermal Stability of New Polymorphs. *Inorganic Materials*, Vol. 37, No. 9, pp. 953-959, ISSN 0020-1685

Gahr, K.Z.; Blattner, R.; Hwang, D. & Pöhlmann, K. (October 2001). Micro- and macro-tribological properties of SiC ceramics in sliding contact. *Wear*, Vol. 250, No. 1-12, pp. 299 - 310, ISSN 0043-1648

Guicciardi, S.; Sciti, D.; Melandri, C. & Pezzotti, G. (February 2007). Dry sliding wear behavior of nano-sized SiC pins against SiC and Si_3N_4 discs. *Wear*, Vol. 262, No. 5-6, pp. 529 - 535, ISSN 0043-1648

Hall, H.T. (February 1960). Ultra-High-Pressure, High-Temperature Apparatus: the "Belt". *Review of Scientific Instruments* , Vol. 31, No. 2, pp. 125-131, ISSN 0034-6748

Hirano, T. & Niihara, K. (March 1995). Microstructure and mechanical properties of Si_3N_4/SiC composites. *Materials Letters*, Vol. 22, No. 5-6, pp. 249 - 254, ISSN 0167-577X

Khvostantsev, L.G.; Slesarev, V.N. & Brazhkin, V.V. (2004). Toroid type high-pressure device: history and prospects. *High Pressure Research*, Vol. 24, No. 3, pp. 371-383, ISSN

Kim, Y.; Lee, Y. & Mitomo, M. (August 2006). Sinterability of Nano-Sized Silicon Carbide Powders. *Journal of the Ceramic Society of Japan*, Vol. 114, No. 1332, pp. 681-685, ISSN 0914-5400

Kinoshita, T.; Munekawa, S. & Tanaka, S.I. (February 1997). Effect of grain boundary segregation on high-temperature strength of hot-pressed silicon carbide. *Acta Materialia*, Vol. 45, No. 2, pp. 801 - 809, ISSN 1359-6454

Lee, S.M.; Kim, T.W.; Lim, H.J.; Kim, C.; Kim, Y.W. & Lee, K.S. (May 2007). Mechanical Properties and Contact Damages of Nanostructured Silicon Carbide Ceramics. *Journal of the Ceramic Society of Japan*, Vol. 115, No. 1341, pp. 304-309, ISSN 0914-5400

Lojanová, S.; Tatarko, P.; Chlup, Z.; Hnatko, M.; Dusza, J.; Lencés, Z. & Sajgalík, P. (July 2010). Rare-earth element doped Si_3N_4/SiC micro/nano-composites--RT and HT mechanical properties. *Journal of the European Ceramic Society*, Vol. 30, No. 9, pp. 1931 - 1944, ISSN 0955-2219

Magnani, G.; Minoccari, G. & Pilotti, L. (June 2000). Flexural strength and toughness of liquid phase sintered silicon carbide. *Ceramics International*, Vol. 26, No. 5, pp. 495 - 500, ISSN 0272-8842

Manghnani, M.; Ming, L. & Jamieson, J. (November 1980). Prospects of using synchrotron radiation facilities with diamond-anvil cells: High-pressure research applications in geophysics. *Nuclear Instruments and Methods*, Vol. 177, No. 1, pp. 219 - 226, ISSN 0029-554X

Murthy, V.S.R.; Kobayashi, H.; Tamari, N.; Tsurekawa, S.; Watanabe, T. & Kato, K. (July 2004). Effect of doping elements on the friction and wear properties of SiC in unlubricated sliding condition. *Wear*, Vol. 257, No. 1-2, pp. 89 - 96, ISSN 0043-1648

Niihara, K.; Kusunose, T.; Kohsaka, S.; Sekino, T. & Choa, Y.H. (1999). Multi-Functional Ceramic Composites trough Nanocomposite Technology. *Key Engineering Materials* , Vol. 161-163, No. , pp. 527-534, ISSN 1013-9826

Piermarini, G.J. (2008). Diamond Anvil Cell Techniques, In: *Static Compression of Energetic Materials*, S.M. Peiris & G.J. Piermarini, (Eds.), 1-74, Springer, ISBN 978-3-540-68146-5, Berlin Heidelberg, Germany

Prikhna, A. (February 2008). High-pressure apparatuses in production of synthetic diamonds (Review). *Journal of Superhard Materials*, Vol. 30, No. 1, pp. 1-15, ISSN 1063-4576

Richerson, D.W. (2004). Advanced ceramic materials, In: *Handbook of advanced materials*, J.K. Wessel, (Ed.), 65-88, John Wiley & Sons, Inc., ISBN 0-471-45475-3, Hoboken, New Jersey, USA

Sajgalík, P.; Hnatko, M.; Lofaj, F.; Hvizdos, P.; Dusza, J.; Warbichler, P.; Hofer, F.; Riedel, R.; Lecomte, E. & Hoffmann, M.J. (April 2000). SiC/ Si_3N_4 nano/micro-composite -- processing, RT and HT mechanical properties. *Journal of the European Ceramic Society*, Vol. 20, No. 4, pp. 453 - 462, ISSN 0955-2219

Suyama, S.; Kameda, T. & Itoh, Y. (March-July 2003). Development of high-strength reaction-sintered silicon carbide. *Diamond and Related Materials*, Vol. 12, No. 3-7, pp. 1201 - 1204, ISSN 0925-9635

Takahashi, K.; Jung, Y.; Nagoshi, Y. & Ando, K. (June 2010). Crack-healing behavior of Si_3N_4/SiC composite under stress and low oxygen pressure. *Materials Science and Engineering: A*, Vol. 527, No. 15, pp. 3343 - 3348, ISSN 0921-5093

Tanaka, H.; Hirosaki, N. & Nishimura, T. (December 2003). Sintering of Silicon Carbide Powder Containing Metal Boride. *Journal of the Ceramic Society of Japan*, Vol. 111, No. 1300, pp. 878-882, ISSN 0914-5400

Xu, C. (2005). Effects of particle size and matrix grain size and volume fraction of particles on the toughening of ceramic composite by thermal residual stress. *Ceramics International*, Vol. 31, No. 4, pp. 537 - 542, ISSN 0272-8842

Yamada, K. & Kamiya, N. (March 1999). High temperature mechanical properties of Si_3N_4-MoSi2 and Si_3N_4-SiC composites with network structures of second phases. *Materials Science and Engineering A*, Vol. 261, No. 1-2, pp. 270 - 277, ISSN 0921-5093

Yeomans, J. (2008). Ductile particle ceramic matrix composites--Scientific curiosities or engineering materials?. *Journal of the European Ceramic Society*, Vol. 28, No. 7, pp. 1543-1550, ISSN 0955-2219

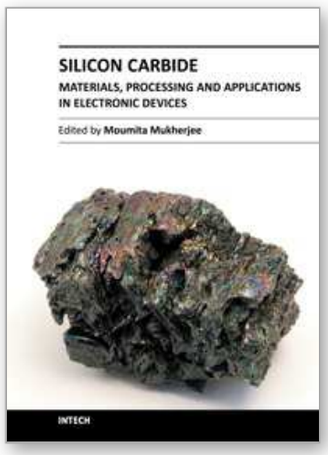

Silicon Carbide - Materials, Processing and Applications in Electronic Devices

Edited by Dr. Moumita Mukherjee

ISBN 978-953-307-968-4
Hard cover, 546 pages
Publisher InTech
Published online 10, October, 2011
Published in print edition October, 2011

Silicon Carbide (SiC) and its polytypes, used primarily for grinding and high temperature ceramics, have been a part of human civilization for a long time. The inherent ability of SiC devices to operate with higher efficiency and lower environmental footprint than silicon-based devices at high temperatures and under high voltages pushes SiC on the verge of becoming the material of choice for high power electronics and optoelectronics. What is more important, SiC is emerging to become a template for graphene fabrication, and a material for the next generation of sub-32nm semiconductor devices. It is thus increasingly clear that SiC electronic systems will dominate the new energy and transport technologies of the 21st century. In 21 chapters of the book, special emphasis has been placed on the â€œmaterialsâ€ aspects and developments thereof. To that end, about 70% of the book addresses the theory, crystal growth, defects, surface and interface properties, characterization, and processing issues pertaining to SiC. The remaining 30% of the book covers the electronic device aspects of this material. Overall, this book will be valuable as a reference for SiC researchers for a few years to come. This book prestigiously covers our current understanding of SiC as a semiconductor material in electronics. The primary target for the book includes students, researchers, material and chemical engineers, semiconductor manufacturers and professionals who are interested in silicon carbide and its continuing progression.

INTECH
open science | open minds

InTech Europe
University Campus STeP Ri
Slavka Krautzeka 83/A
51000 Rijeka, Croatia
Phone: +385 (51) 770 447
Fax: +385 (51) 686 166

InTech China
Unit 405, Office Block, Hotel Equatorial Shanghai
No.65, Yan An Road (West), Shanghai, 200040, China
中国上海市延安西路65号上海国际贵都大饭店办公楼405单元
Phone: +86-21-62489820
Fax: +86-21-62489821

IntechOpen

IntechOpen